DOI: 10.1002/cbic.201200397

Single Labeled DNA FIT Probes for Avoiding False-Positive Signaling in the Detection of DNA/RNA in qPCR or Cell Media

Felix Hövelmann, Lucas Bethge, and Oliver Seitz*[a]

Oligonucleotide hybridization probes that fluoresce upon binding to complementary nucleic acid targets allow the real-time detection of DNA or RNA in homogeneous solution. The most commonly used probes rely on the distance-dependent interaction between a fluorophore and another label. Such dual-labeled oligonucleotides signal the change of the global conformation that accompanies duplex formation. However, undesired nonspecific binding events and/or probe degradation also lead to changes in the label–label distance and, thus, to ambiguities in fluorescence signaling. Herein, we introduce singly labeled DNA probes, "DNA FIT probes", that are designed to avoid false-positive signals. A thiazole orange (TO) intercalator dye serves as an artificial base in the DNA probe. The probes show little background because the attachment mode hinders 1) interactions of the "TO base" in *cis* with the disordered nucleobases of the single strand, and 2) intercalation of the "TO nucleotide" with double strands in *trans*. However, formation of the probe–target duplex enforces stacking and increases the fluorescence of the TO base. We explored open-chain and carbocyclic nucleotides. We show that the incorporation of the TO nucleotides has no effect on the thermal stability of the probe–target complexes. DNA and RNA targets provided up to 12-fold enhancements of the TO emission upon hybridization of DNA FIT probes. Experiments in cell media demonstrated that false-positive signaling was prevented when DNA FIT probes were used. Of note, DNA FIT probes tolerate a wide range of hybridization temperature; this enabled their application in quantitative polymerase chain reactions.

Introduction

Fluorescent nucleobases and base surrogates provide interesting opportunities.[1,2] Environmentally sensitive fluorophores have been positioned within the base stack of DNA to probe the local structure and dynamics of nucleic acids,[3] to detect DNA–protein interactions, and to construct helical fluorophore clusters.[4–5] One important aim of these investigations has been to develop DNA diagnostic probes that experience enhancement of fluorescence emission upon hybridization with complementary DNA or RNA targets.[6] Such probes will be useful for the real-time detection of DNA or RNA in complex environments such as PCR mixtures,[7] cell lysates, or even live cells.[8] The majority of DNA detection methods used in applications rely on the distance-dependent interaction between two fluorophores. However, ambiguities in fluorescence signaling can arise when probe degradation and/or unintended binding of probes to proteins induce changes in fluorophore–fluorophore distance.[9–10] The use of a single fluorophore probes should provide a solution to this problem and, in addition, should confer advantages as far as cost-effectiveness is concerned. Nevertheless, there are only a few examples wherein singly labeled probes show the properties required to reduce background in complex biomolecular environments, that is, 1) visible-light-excitable fluorophores and 2) substantial ($\geq$ fivefold) increases in fluorescence upon binding of complementary targets.[11]

Recently, we introduced the so-called FIT (forced intercalation) probes, wherein a canonical nucleobase in a peptide nucleic acid (PNA) oligomer is exchanged for a single thiazole orange (TO).[12] The TO dye belongs to a family of DNA intercalators which have low fluorescence in the free form because twisting motions around the central methine bridge lead to rapid depletion of the TO excited state.[13] In the DNA-bound form, twisting is hampered and fluorescence is dramatically enhanced. PNA FIT probes have useful properties. These probes show weak fluorescence in the single-stranded state. Hybridization with fully complementary DNA or RNA is accompanied by strong enhancements of fluorescence.[14] Of note, PNA FIT probes discriminate single-base mismatches under condition where both matched and single mismatched probe–target complexes form, because the TO-base surrogate fluoresces only weakly when the neighboring base pair is mismatched. We applied the PNA FIT probes in real-time PCR-based genotyping and in the live cell imaging of viral mRNA.[15,16] Other laboratories have confirmed the interesting properties of PNA FIT probes in RNA hybridization studies and in the imaging of microRNA or mRNA in living cells.[17]

Though PNA-based probes offer advantages as far as stability in biological environments and ease of synthetic modifica-

[a] *F. Hövelmann, Dr. L. Bethge, Prof. Dr. O. Seitz*
Institut für Chemie der Humboldt-Universität zu Berlin
Brook-Taylor Strasse 2, 12489 Berlin (Germany)
E-mail: oliver.seitz@chemie.hu-berlin.de

Supporting information for this article is available on the WWW under http://dx.doi.org/10.1002/cbic.201200397.

tions are concerned, there are drawbacks.[18] The known protocols for cell transfection or enzymatic modification cannot be applied, and PNA synthesis is, currently, more costly than DNA synthesis. We set out to develop a DNA version of FIT probes. Herein we describe the synthesis and properties of DNA-based probes in which a member of the family of the thiazole orange based intercalator dyes serves as a fluorescent base surrogate. In contrast to previously published probes from Asseline,[19] Wagenknecht,[20] and Okamoto,[21] the involvement of flexible linkers between the TO dye and the DNA scaffold is avoided.

Rather, we present a new cyclic building block (**cRib(TO)**, Scheme 1), in which the flexibility of the TO–backbone linkage is significantly reduced. We show that the replacement of

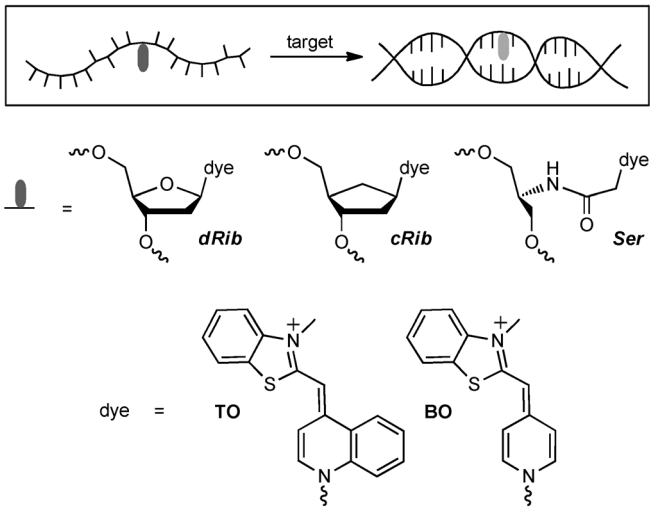

Scheme 1. DNA FIT probes and fluorogenic nucleotides synthesized in this study.

a canonical nucleobase by the TO dye in DNA FIT probes has no effect on the thermal stability of probe–target complexes. The turn-on of TO emission upon hybridization of DNA FIT probes is observed with both DNA and RNA targets. To demonstrate the usefulness of the DNA-based FIT probes, we explored applications such as quantitative PCR (qPCR) analysis and RNA detection in cell lysates.

Results and Discussion

Previous studies on PNA and DNA probes had indicated that the linker connecting the TO fluorochrome with the scaffold has a critical influence on the fluorescence properties. For example, PNA probes in which TO was tethered at carboxyethylene or carboxypentamethylene groups to aminoethylglycine failed to show the desired turn-on of fluorescence upon hybridization.[12c] A similar behavior was observed when carboxyethylene rather than carboxymethylene was used to anchor TO at an L-serinol nucleotide in DNA probes.[22] We assumed that the hypothesized "dTO-nucleoside" **dRib(TO)** would provide the rigidity required to improve the enforced intercalation in DNA-based FIT probes (Scheme 1). However, the N-glycosidic bond in **dRib(TO)** is extremely labile. The carbocyclic 2′-deoxyribose analogue **cRib(TO)** was expected to confer stability required for automated DNA synthesis yet retain the characteristic of the cyclic scaffold.

Synthesis

The L-serinol-linked TO-nucleotide **7** was previously described (Scheme 2).[22] The synthesis of the carbocyclic nucleotides **6α** and **6β** was commenced from dicyclopentadiene, which, in accordance with a procedure published by Meier, was converted in a sequence of benzyloxymethylation and hydroboration reactions into 4a′-carba-α-(D)-5′,3′-dibenzyl-2′-deoxyribose **1**.[23] The unprotected hydroxy group in **1** was converted to produce the mesylate **2**. The reaction of **2** with neat 4-methyl quinoline (tenfold excess) at 90 °C over a period of 40 h fol-

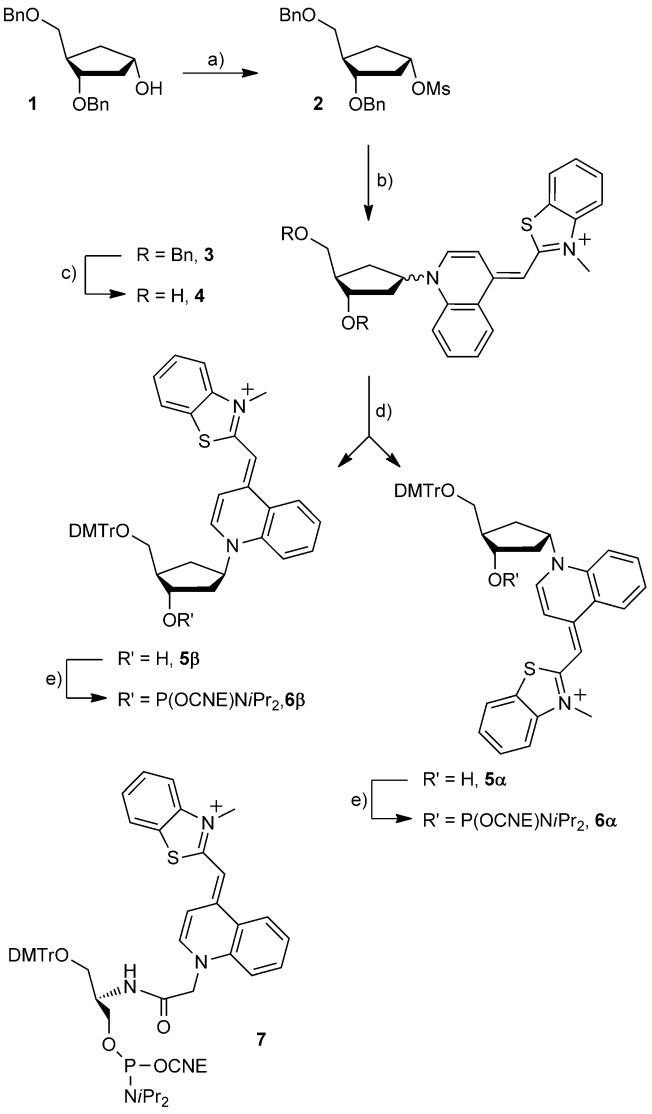

Scheme 2. a) MsCl, NEt_3, CH_2Cl_2, 93%; b) i: 4-methyl quinoline, 90 °C; ii: 3-methyl-2-(methylthio)benzothiazolium tosylate, NEt_3, 36% (2 steps); c) BBr_3, CH_2Cl_2, quant.; d) DMTrCl, $EtNiPr_2$, pyridine, KPF_6, 85%; e) 2-cyanoethyl *N*,*N*-diisopropylchloro phosphoramidites, $EtNiPr_2$, CH_2Cl_2, quant.

lowed by addition of 2-methylthiobenzothiazolium tosylate in the presence of NEt_3 yielded **3** as a mixture of diastereomers. The removal of the benzyl protecting groups proceeded smoothly when BBr_3 was used. The subsequent introduction of the DMTr protecting group proved challenging because of the poor solubility of **4** in pyridine, DMF, or acetonitrile. However, the addition of KPF_6 and the resulting exchange of the counter ion in **4** solved the solubility problem. Under these conditions the DMTr protection succeeded in 85% yield. After chromatographic separation of the two diastereomers, **5α** and **5β** isomers were separately converted to the phosphoamidites **6α** and **6β**.

The phosphoramidites (**6α**, **6β**, and **7**) were dissolved in dry MeCN and used in automated DNA synthesis.[24] The coupling time for the TO-containing building blocks was prolonged to 3 min. This resulted in up to 99% coupling yield (Figure S1 in the Supporting Information). Cleavage was achieved by employing fast deprotection of dG(dmf) (32% NH_3 (aq.), 2 h, 55 °C).

Duplex stability

Our main interest pertains to the detection of RNA in complex environments, such as cell lysates and living cells. Therefore, we investigated the hybridization of DNA FIT probes with RNA targets. We first assessed the effect of the TO modification on the thermal stability of probe–target duplexes. In a set of 18-mer DNA FIT probes directed against different segments of β-actin (nt 1138–1163) from Madin–Darby canine kidney (MDCK) cells, the TO nucleotides (**6α**, **6β**, and **7**) were placed at central positions.[25] After addition of the complementary RNA target (**RNA1**) the thermal stability was evaluated by means of UV-monitored melt analysis (Table 1). A comparison with the unmodified oligonucleotides **ON1**–**ON3** revealed marginal destabilization of the formed duplexes when the open-chain serinol nucleotide **Ser(TO)** or the β-configured carbocyclic nucleotide **βcRib(TO)** was involved. For these TO placements, disruption of AT base pairs in **ON1X** and **ON3X** led to a somewhat weaker effect ($\Delta T_m \approx -1$ °C) than disruption of a GC base pair in **ON2X** ($\Delta T_m \approx -3$ °C). Of note, the α-carbocyclic TO-nucleotide **αcRib(TO)** conferred a significant stabilization to the DNA–RNA duplex. We concluded that the introduction of a TO nucleotide in DNA FIT probes does not significantly affect, if at all, the affinity for the targeted RNA.

Table 1. Melting temperatures of DNA FIT probes directed against a segment of RNA coding for β-actin in MDCK cells.[a]

ON	Sequence 5′→3′	T_M [°C] X=Ser(TO)	X=βcRib(TO)	X=αcRib(TO)
1X	CACAGAGTXCTTGCGCTC	60.0	59.5	66.0
1	CACAGAGTACTTGCGCTC	60.5		
2X	ACAGAGTAXTTGCGCTCA	56.3	54.0	61.3
2	ACAGAGTACTTGCGCTCA	58.0		
3X	CAGAGTACXTGCGCTCAG	62.0	62.0	66.3
3	CAGAGTACTTGCGCTCAG	63.0		

[a] Target RNA: CACCCC CUGAGC GCAAGU ACUCUG UGU (**RNA1**). Conditions: 1 μM probe and 1 μM **RNA1** in PBS (10 mM Na_2HPO_4, 100 mM NaCl, pH 7), absorption 260 nm.

Fluorescence properties

The fluorescence of probes **ON1X**–**ON3X** was measured before and after addition of target RNA. Figure 1 shows fluorescence spectra and fluorescence enhancements I/I_0 (where I_0 and I are the fluorescence intensities of the single-stranded form and the double-stranded form, respectively). The α-carbocyclic linkage exhibited only modest enhancements of TO emission (≤ twofold) upon hybridization. By contrast, the β-carbocylic TO nucleotide in **ON3X** provided the highest hybridization-induced intensification of fluorescence ($I/I_0 = 12$) among the sequences tested. The serinol-linked TO nucleotide proved least sensitive to the sequence environment and showed a useful average $I/I_0 \approx 7$.

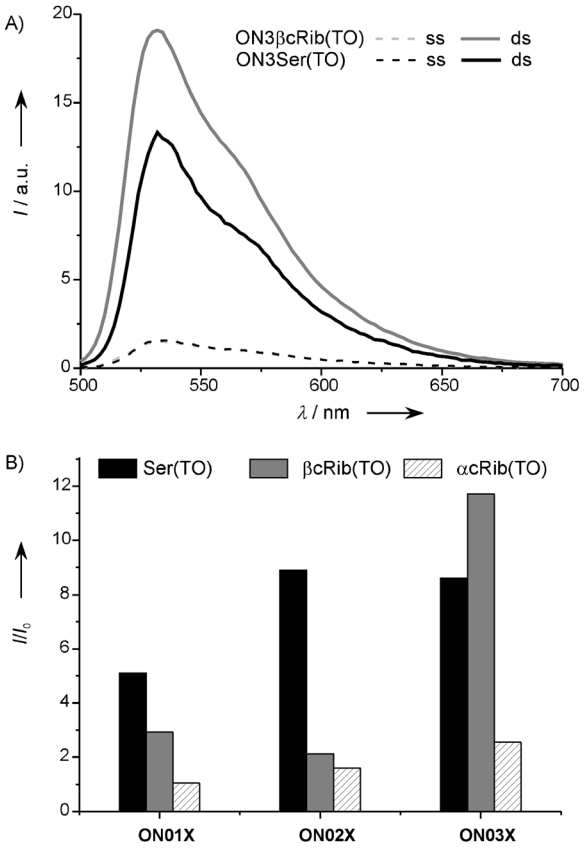

Figure 1. A) Fluorescence spectra of **ON3X** (black: X=**Ser(TO)**, gray: X=**βcRib(TO)**) before (dashed) and after (solid) addition of **RNA1**. B) Fluorescence enhancement at 535 nm of **ON1X**–**ON3X** upon addition of **RNA1**. Conditions: 1 μM probe in PBS (10 mM Na_2HPO_4, 100 mM NaCl, pH 7) and 5 μM RNA target; when added, 37 °C, λ_{ex}=485 nm.

Two conclusions can be drawn from these experiments. First, there is no correlation between duplex stability and fluorescence responsiveness of DNA FIT probes. Second, though

the β-carbocyclic TO nucleotide might provide the highest fluorescence enhancement, it was the serinol-linked TO nucleotide which appeared more robust in this sequence context. This and its ease of synthesis prompted further investigations of the serinol-linked TO nucleotide.

We explored the open-chain TO nucleotide within another sequence context and selected a 27-nucleotide segment of mRNA coding for neuraminidase (NA) of the H1N1 influenza A/PR/8 virus (nucleotides 582–608).[26] This target segment was first studied by Wang et al. by using molecular beacon probes.[27] A "TO walk" was used to explore the dependence of the fluorescence properties on the immediate neighbors (Table 2). A useful fluorescence enhancement ($I/I_0 \geq 5$) upon

Table 2. Fluorescence enhancement of DNA FIT probes directed against mRNA coding for neuraminidase of H1N1 influenza A/PR/8.

ON	Sequence 5′→3′	I/I_0[a]
4	GGTTTC Ser(TO) GTTATTATGCCGTTGTATTT	7
5	GGTTTCA Ser(TO) TTATTATGCCGTTGTATTT	6
6	GGTTTCAG Ser(TO) TATTATGCCGTTGTATTT	12
7	GGTTTCAGT Ser(TO) ATTATGCCGTTGTATTT	4
8	GGTTTCAGTT Ser(TO) TTATGCCGTTGTATTT	11
9	GGTTTCAGTTA Ser(TO) TATGCCGTTGTATTT	5
10	GGTTTCAGTTAT Ser(TO) ATGCCGTTGTATTT	2
11	GGTTTCAGTTATT Ser(TO) TGCCGTTGTATTT	6
12	GGTTTCAGTTATTA Ser(TO) GCCGTTGTATTT	1
13	GGTTTCAGTTATTAT Ser(TO) CCGTTGTATTT	3
14	GGTTTCAGTTATTATG Ser(TO) CGTTGTATTT	5
15	GGTTTCAGTTATTATGC Ser(TO) GTTGTATTT	7
16	GGTTTCAGTTATTATGCC Ser(TO) TTGTATTT	10
17	GGTTTCAGTTATTATGCCG Ser(TO) TGTATTT	12
18	GGTTTCAGTTATTATGCCGT Ser(TO) GTATTT	3

[a] Target: **RNA2**, AAAUACAACGGCAUAAUAACUGAAACC. Conditions: see Figure 1.

RNA hybridization was provided by 10 of the 15 single TO-labeled probes tested. Four probes showed $I/I_0 \geq 10$. Probe **ON6** proved the most responsive and was found to signal the presence of the complementary RNA target with a 12-fold enhancement of fluorescence. For comparison, RNA hybridization of the molecular beacon **MB1**, which was recently employed to detect influenza mRNA in living cells, was accompanied by sixfold intensification of fluorescence.[27]

Comparison between DNA FIT probe and DNA molecular beacon in cell lysate

The use of nucleic acid-based probes in complex biological samples such as cell lysate or live cells is challenging. Nonspecific binding to DNA- or RNA-binding proteins and/or degradation by nucleases can increase background. These problems are pertinent to fluorophore/quencher-labeled DNA probes. For example, undesired protein binding or degradation of DNA molecular beacon probes will separate the fluorophore from the quencher and will cause increases in fluorescence in the absence of target.[28] By contrast, DNA FIT probes operate by a different signaling mechanism. Rather than the global changes in conformation reported by DNA molecular beacons, the single TO dye senses changes of the local environment.[22] As a result, the TO nucleotide will not fluoresce upon scission of the phosphodiester backbone. Strong fluorescence emission will occur when the TO nucleotide stacks with the base pairs formed upon probe–target recognition. This binding mode is not available with proteins. Thus, we assumed that DNA FIT probes are less vulnerable to false-positive signaling.

We compared the DNA FIT probe (Figure 2A) and the DNA molecular beacon designs (Figure 2B) and addressed the two major sources of high background in complex biological environments, that is, 1) nonspecific binding and 2) enzymatic digestion of the probe. The probes were dissolved in phosphate

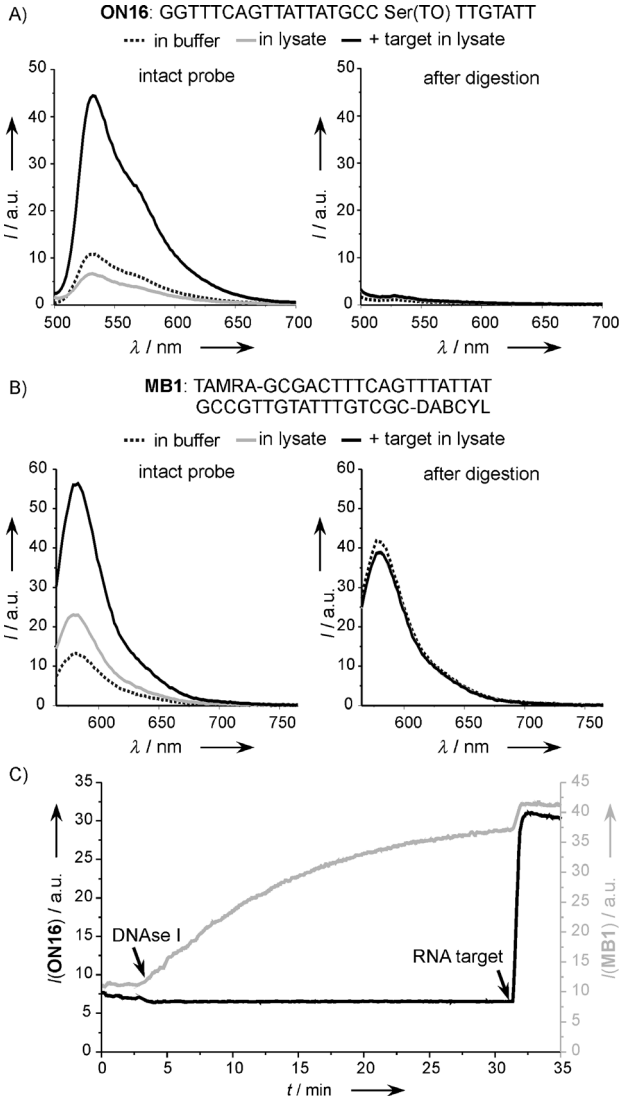

Figure 2. Relative fluorescence spectra of A) **ON17** and B) **MB1** in PBS (dotted), cell lysate (gray) and after addition of complementary RNA target (**RNA2**) in cell lysate (black) for intact probe (left) and after complete digestion (right) with DNase I (0.44 mg mL^{-1}) for 1 h at 37 °C. Conditions: A), B) see Figure 1, $\lambda_{ex} = 550$ nm for detection of **MB1**. C) Time-dependent fluorescence of **MB1** (gray) and **ON16** (black) in PBS after addition of DNase I (0.05 mg mL^{-1} at 3 min) and **RNA2** (at 31 min). Conditions: 0.1 μM probe in PBS, 0.5 μM **RNA2** when added, 37 °C, $\lambda_{em} = 535$ nm or $\lambda_{em} = 580$ nm for detection of **ON16** or **MB1**, respectively.

buffered saline (PBS) or crude lysate from MDCK cells, and the fluorescence was measured before and after addition of RNA target. The change from the PBS buffer to cell lysate was accompanied by an increase in the fluorescence of the unbound **MB1** probe (Figure 2B). This increase in background resulted in reduced responsiveness to target addition (I/I_0 (cell lysate) = $0.65 \times I/I_0$ (PBS buffer)). In contrast, DNA FIT probe **ON16** fluoresced with lower intensity in cell lysate than in PBS (Figure 2A). We speculate that collisional quenching by cellular components or a better solubilization of the TO dye might contribute to the reduced fluorescence intensity in cell lysate. Regardless of the mechanism involved, the DNA FIT probe **ON16** remained highly responsive in cell lysate.

Next studied was the behavior of probes after degradation by nucleases. Both DNA FIT probe **ON16** and DNA molecular beacon probe **MB1** were digested by treatment with DNase I (40 μL, 0.44 mg mL^{-1}, ≥2000 U mg^{-1}, 1 h, 37 °C). The digested probes were added to phosphate buffer or cell lysate. The DNA FIT probe exhibited insignificant fluorescence in both media (Figure 2A, right). It was impossible to distinguish TO emission from the lysate-only background fluorescence. This experiment proved that the remnants of probe digestion (e.g., TO nucleoside) stained neither cellular DNA nor RNA. As expected for complete probe digestion, the fluorescence signal remained unaltered when complementary RNA target was added. The **MB1** probe showed the opposite behavior (Figure 2B, right). Degradation resulted in false-positive signaling as evidenced by increases in fluorescence (70% in lysate, 220% in PBS) in the absence of RNA target.

To assess the vulnerability to nuclease degradation, MB probe **MB1** and DNA FIT probe **ON17** were jointly dissolved in PBS buffer, and a diluted DNase I solution (5 μL, 0.05 μg mL^{-1}) was added. The signal for MB fluorescence immediately increased (Figure 2C). The addition of target RNA showed that the MB beacon lost 90% of its responsiveness after 30 min of incubation in cell lysate spiked with DNase I, whereas the DNA FIT probe lost only 20% of its responsiveness, as inferred from the 5.4-fold increase in TO emission upon addition of RNA target. From this data we concluded that DNA FIT probes have higher resistance to nuclease cleavage than DNA MB probes, possibly because the sequence internal modification hinders attack by endonucleases.

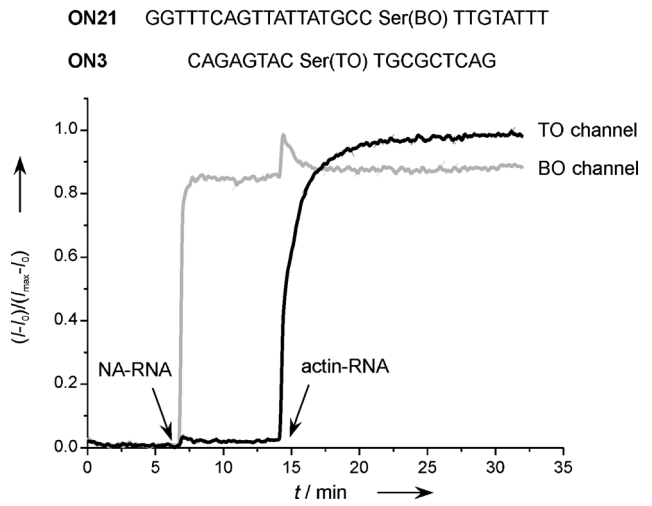

Figure 3. Simultaneous measurement of time-dependent fluorescence of **ON21** and **ON3 Ser(TO)** after addition of NA RNA (**RNA2**, 7 min) and actin RNA (**RNA1**, 14 min). Conditions: 0.1 μM probes in lysate of 10^5 MDCK cells in 150 μL lysis buffer (50 mM Tris·HCl, 150 mM NaCl, 0.8% PN-40, pH 7.4) and 0.5 μM RNA target when added, 37 °C, black: TO channel, λ_{ex} = 515 nm, λ_{em} = 535 nm; gray: BO channel, λ_{ex} = 460 nm, λ_{em} = 480 nm.

synthesized the L-serinol(BO) **8** and the carbocyclic BO nucleotide building blocks **9α** and **9β** (Scheme 3; synthesis shown in Schemes S1 and S2) and introduced the BO nucleotide into DNA probes **ON19X**–**ON21X** (Table S1). These probes were complementary to a segment from the mRNA coding for NA of the H1N1 influenza A/PR/8 virus.[26]

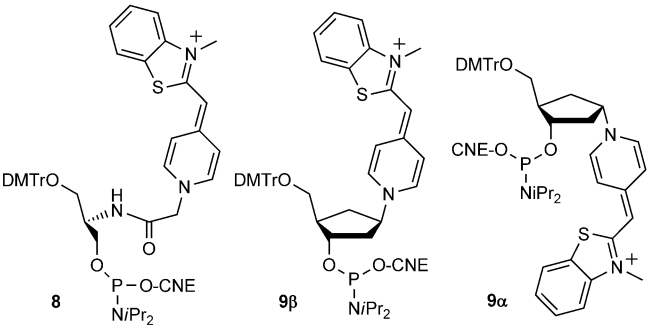

Scheme 3. Synthesized BO nucleotides.

Dual-color RNA detection

The simultaneous detection of two different RNA targets would greatly facilitate the analysis of gene expression, for example, when one probe serves as a positive control for expression of a housekeeping gene while the other probe responds to the expression of the target gene. This requires two spectrally resolvable dyes. Previous investigations with PNA probes had shown that the "FIT concept" extends to other members of the thiazole orange family of asymmetric cyanine dyes.[29] The fluorescence spectra of TO and BO dyes are resolvable (Figure S5). It should thus be possible to selectively monitor BO fluorescence (λ_{ex} = 460 nm, λ_{em} = 480 nm) with only little crosstalk with TO fluorescence (λ_{ex} = 515 nm, λ_{em} = 535 nm). We

The NA-specific BO probe **ON21** was combined in phosphate buffer with the actin-specific TO probe **ON3Ser(TO)**. Control experiments confirmed that the enhancement of BO emission required the presence of NA RNA (Figure S5). Analogously, enhancements of TO emission only occurred when actin RNA was added. To assess the hybridization behavior of the DNA FIT probes in complex biomolecular environments, we performed kinetic measurements in crude lysate from MDCK cells (Figure 3). NA RNA (**RNA2**) was added after 7 min equilibration. The signal measured in the BO channel increased almost instantaneously. The negligible response in the TO channel attested to the selectivity of fluorescence signaling.

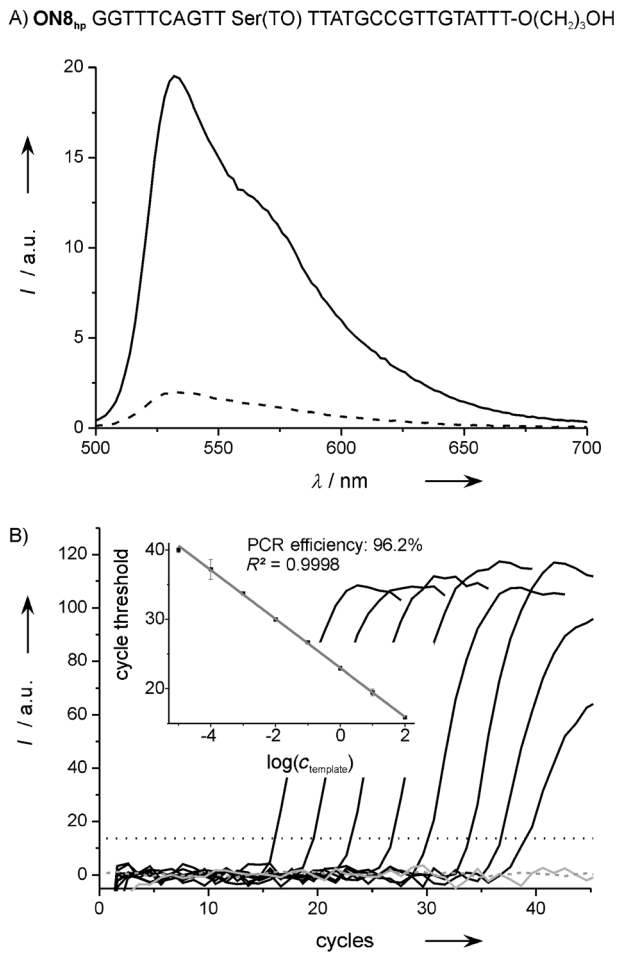

Figure 4. A) Fluorescence emission of **ON8$_{hp}$** in PBS before (dashed) and after (solid) addition of complementary DNA. Conditions: 1 μM probe in PBS buffer and 5 μM DNA target when added, 57.5 °C, λ_{ex} = 485 nm. B) **ON8$_{hp}$** in qPCR analysis of cDNA (100 ng μL^{-1}–10 fg μL^{-1}, black solid lines) obtained from H1N1 infected MDCK cells; no-template controls (gray solid) and cDNA (10 ng μL^{-1}, gray dashed) from non-infected cells. The dotted line shows the threshold value used for the calibration curve (inset).

Nevertheless, the TO signal immediately responded when actin RNA (**RNA1**) was added. A small but measurable increase in the BO signal faded within 3 min. These experiments revealed 1) the high specificity of dual-color RNA detection, and 2) the high response rates of the DNA FIT probes.

qPCR analysis

Gene expression is commonly analyzed by means of qPCR and fluorogenic hybridization probes that report on the amplification of a target sequence. We assessed whether DNA FIT probes also enable the detection of DNA produced by PCR. This would facilitate the comprehensive analysis of gene expression. We analyzed cDNA that had been obtained through reverse transcription of mRNA isolated from MDCK cells after infection with the influenza A/PR/8 virus. The aim was to quantify mRNA coding for NA of the influenza A virus. A highly responsive DNA FIT probe from the TO walk shown in Table 2 was selected in order to study the fluorescence properties upon hybridization with complementary DNA. A 3′ cap was introduced onto probe **ON8** to avoid extension during PCR. For this purpose, the DNA FIT probe was synthesized on propane-1,3-diol-premodified controlled-pore glass (CPG; see the Supporting Information). Hybridization of the 3′-hydroxypropyl modified FIT probe **ON8$_{hp}$** with target DNA at 57.5 °C led to tenfold enhancement of the TO emission intensity (Figure 4A). The qPCR experiments were performed with NA-specific primers, and the fluorescence of the FIT probe was read in the FAM (fluorescein) channel. Figure 4B shows the amplification curves for a cDNA dilution series.

The resulting calibration curve (Figure 4B, inset) revealed a high PCR efficiency (96%) and a linear measuring range over at least eight orders of magnitude. Control experiments carried out without cDNA (no template control, NTC) or with cDNA obtained from non-infected cells showed that the DNA FIT probe **ON8$_{hp}$** avoided false-positive signaling in the PCR assay. Thus, in contrast to nonspecific stains, such as SYBR Gold (Figure S6), DNA FIT probes do not detect primer dimers, which are formed in the late stage of PCR (> 30 cycles).

Discussion

This work was motivated by the increasing importance that has been assigned to studies of RNA expression. It was our aim to explore whether single fluorophore-labeled DNA FIT probes enable RNA detection in complex environments such as cell lysates. The design of DNA FIT probes is different from other reported single-label hybridization probes. In most probes, the sensor dye is attached at the periphery of the probe or by flexible linkers. For example, Wagenknecht and Asseline have attached TO to internal positions with flexible linkers.[19,20,30] A similar tactic has been applied for the labeling in HyBeacons.[31] Light-Up probes contain TO at a terminal position of PNA.[11c] In Okamoto's ECHO probes and Saito's base-discriminating nucleotides, the sensor dye hangs from the base periphery.[11b] As few of these probes provide significant (≥ fivefold) increases in fluorescence upon hybridization, it remains difficult to detect RNA behind the background of the plethora of biomolecules present in cell lysate. Interactions of the sensor dye with other biomolecules or biomolecular aggregates must be avoided, or must not lead to fluorescence enhancement. We believe that the attachment mode realized in DNA FIT probes sterically shields the TO dye from interactions with non-targets. Indeed, the experiments in cell media demonstrated that DNA FIT probes such as **ON16** show no sign of false-positive signaling.

We explored two TO attachment modes. Because of the robustness of the fluorescence response and the ease of preparation, we explored the serinol scaffold in more detail. Tucker has also used this linkage to anchor anthracene to DNA.[33] The "anthracene base" significantly perturbed duplex stability and furnished rather modest fluorescence responsiveness. By contrast, the TO base in DNA FIT probes does not affect the stability of the probe–target duplex and provides high enhancement of TO emission upon hybridization. The DNA FIT probes were designed in analogy to the PNA FIT probes. However, the

usage of a DNA scaffold is more challenging because in the free form TO has affinity for single-stranded and double-stranded DNA as well as for RNA. The steric bulk provided by the serinol-based and carbocylic TO linkages prevents interactions in *cis* and helps decrease the fluorescence of unbound probes.

The experiments with cell media showed that DNA FIT probes can solve specificity problems pertinent to dual-labeled probes, such as the frequently used DNA molecular beacons. Probes that draw on two chromophores and the hybridization-induced change of the global conformation will provide false-positive signals when the two interacting chromophores are separated upon degradation by nucleases or unintended binding to proteins or other biomolecules.[9,10] By contrast, neither degradation nor exposure to crude cell lysate was a source of false-positive signaling when DNA FIT probes were used.

Conclusions

The collected data indicate that singly labeled DNA FIT probes, in which a member of the thiazole orange (TO) family of intercalator dyes occupies the position of a canonical nucleobase, enable fluorescence-based detection of complementary DNA and RNA in complex environments. We explored two modes of attachment. Both the linkage by a carbocyclic scaffold and the linkage by a serinol-based open-chain ribose analogue provided high stability of the probe–target complexes formed. Hybridization to a nucleic acid target was signaled by up to 12-fold enhancement of thiazole orange (TO) emission. Experiments in cell lysate revealed that the fluorescence of the unbound DNA FIT probes remained low. Neither degradation by DNase I nor exposure to crude cell lysate was a source of false-positive signaling. The method extends to other colors. The combined use of a TO nucleotide ($\lambda_{ex}=515$ nm, $\lambda_{em}=535$ nm) and a BO nucleotide ($\lambda_{ex}=460$ nm, $\lambda_{em}=480$ nm) in two different probes enabled the simultaneous, yet fully independent, detection of two RNA model targets in cellular media. Of note, the probes tolerated a wide range of hybridization temperatures, which enabled the application to the qPCR analysis of viral mRNA. A sequence coding for NA of influenza A virus was targeted in a feasibility study. The resulting calibration curve revealed a high sensitivity and a linear measuring range over at least eight orders of magnitude. Thus, the DNA FIT probes are amongst the few fluorogenic hybridization probes that can be used for both the detection of RNA in cell media (and probably also for live-cell RNA imaging) and DNA formed during a polymerase chain reaction. These properties suggest that DNA FIT probes will find applications in other endeavors requiring the real time detection of DNA or RNA in complex samples.

Experimental Section

General information: Reagents were purchased from Sigma–Aldrich, Acros Organics, and TCI-Europe (Zwijndrecht, Belgium). Solvents CH_2Cl_2 and THF were dried by using the SPS-800 solvent purification system (MBraun, Garching, Germany). Dry DMF ($H_2O<0.01\%$) was purchased from Fluka. Aqueous solutions were made with water purified in a Millipore purification device. Column chromatography was performed with SDS 60 ACC silica gel and monitored by TLC with Silica Gel 60 F254 plates (Merck). Optical rotations were measured at the sodium D-line with a model 241 polarimeter (PerkinElmer) with a 100 mm glass cuvette. $[a]_D$ values are given in units of 10^{-1} deg cm^2 g^{-1}. NMR spectra were recorded with a DPX 300 or Avance II 500 spectrometer (Brucker). The signals of the residual protonated solvents ($CDCl_3$, [D$_6$]DMSO, [D$_6$]DMSO/TFA, and CD_3CN) were used as references. Coupling constants are given in hertz. High resolution mass spectra were measured with a QStarXL spectrometer (ESI+; Applied Biosystems). Semipreparative HPLC was carried out on a model 1105 HPLC System (Gilson, Middleton, WI), and analytical RP-HPLC was carried out on the 1105 HPLC and an ACQUITY UPLC System (Waters, Milford, MA). A UV detector ($\lambda=260$ nm) was used for the detection. Semipreparative separations were carried out by using an XBridge BEH130 C18 column (8 μm, 10×150 mm, Waters) at a flow rate of 4 mL min^{-1} at 55 °C. Analytical HPLC was carried out by using an XBridge C18 column (5 μm, 4.6×250 mm; Waters) at a flow rate of 1 mL min^{-1} at 55 °C, or an Acquity BEH300 C18 column (1.7 μm, 2.1×100 mm; Waters) at a flow rate of 0.6 mL min^{-1} at 55 °C. As mobile phase, a binary mixture of A (triethylammonium acetate (TEAA; 0.1 M, pH 7), aq.) and B (acetonitrile) was used. MALDI-TOF mass spectra were measured on Reflex III (Bruker) and Voyager (Applied Biosystems) systems. As matrix we used a mixture of 2,4,6-trihydroxyacetophenone (10 mg in EtOH (1 mL)) and diammonium citrate (50 mg in water (0.5 mL)).

4 a′-Carba-α-(D)-5′,3′-dibenzyl-2′-deoxyribofuranosyl-1′-methylsulfonate (2): NEt_3 (8.73 g, 86.3 mmol, 12.1 mL) was added to a solution of **1** (3.37 g, 10.8 mmol) in dry CH_2Cl_2 (200 mL) at 0 °C under an argon atmosphere. Subsequently, a solution of methanesulfonyl chloride (9.89 g, 86.3 mmol, 6.72 mL) in CH_2Cl_2 (20 mL) was added drop-wise. After one hour, saturated $NaHCO_3$ (aq.) solution (100 mL) was added, and the organic phase was separated. The aqueous layer was extracted with Et_2O (100 mL). The combined organic phases were dried over $MgSO_4$, filtered, concentrated, and further purified by flash column chromatography (cyclohexane/EtOAc 10:1, *v/v*) to yield a colorless oil (3.94 g, 10.1 mmol, 93%). $R_f=0.78$ (EtOAc/cyclohexane 1:1, *v/v*). ^{1}H NMR (300 MHz, $CDCl_3$): $\delta=1.91$ (ddd, $J_1=6.1$, $J_2=8.6$, $J_3=14.4$, 1H; H2′a), 2.13 (m, 1H; H2′b), 2.25 (m, 1H; H4a′a), 2.38 (m, 1H; H4a′b), 2.57 (m, 1H; H4′), 2.98 (s, 3H; CH_3SO_2-), 3.47 (m, 2H; H5′a, H5′b), 3.90 (m, 1H; H3′), 4.51 (m, 4H; 2CH_2), 5.15 (m, 1H; H1′), 7.27–7.39 ppm (10H, m, 10ArCH); ^{13}C NMR (75 MHz, $CDCl_3$): $\delta=35.1$ (C4a′), 38.7 (CH_3), 39.2 (C2′), 44.5 (C4′), 70.8 (C5′), 71.4 (CH_2), 73.1 (CH_2), 80.2 (C3′), 81.8 (C1′), 127.6 (2ArCH), 127.7 (ArCH), 127.7 (ArCH), 127.7 (2ArCH), 128.4 (2ArCH), 128.4 (2ArCH), 138.3 (ArC_q), 138.4 ppm (ArC_q).

4 a′-Carba-α/β-(D)-5′,3′-dibenzyl-2′-deoxyribofuranose(TO) (3): Compound **2** (3.94 g, 10.1 mmol) and 4-methyl quinoline (14.5 g, 101 mmol) were heated to 100 °C for 48 h. After cooling to room temperature, CH_2Cl_2 (200 mL) was added, followed by 3-methyl-2-thiomethyl-benzothiazolium tosylate (7.42 g, 20.1 mmol) and NEt_3 (4.08 g, 40.4 mmol, 5.67 mL). The addition of triethylamine caused an immediate color change to red. After stirring for 4 h under the exclusion of light, the mixture was washed four times with HCl (1 M). The organic layer was dried over $MgSO_4$, filtered, and concentrated. The residue was further purified by flash column chromatography (CH_2Cl_2/MeOH 90:10, *v/v*) to yield a red solid (2.10 g, 2.78 mmol, 36%, ratio of diastereomers $\alpha/\beta=1:1.5$). $R_f=0.53$ (CH_2Cl_2/MeOH/NEt_3 90:10:0.1, *v/v/v*); ^{1}H NMR (300 MHz, $CDCl_3$, 2 diastereomers: $\delta=1.72$ (m, 1H), 2.10 (m, 2H), 2.21 (s, 6H; Ts-CH_3), 2.31 (m, 2H), 2.53 (m, 5H,), 3.45 (m, 4H; 2H5′a, 2H5′b), 3.77 (m,

6H; 2N$^+$CH$_3$), 3.99 (m, 2H; 2H3′), 4.44 (m, 8H; 4Bn-CH$_2$), 4.94 (m, 1H; H1′), 5.10 (m, 1H; H1′), 6.61 (s, 2H; 2-CH=), 7.02–7.62 (m, 40H), 7.88 (m, 4H; 4Ts-H), 8.57 (m, 3H; 3TO-H), 8.80 ppm (m, 1H; 1TO-H); ^{13}C NMR (75 MHz, CDCl$_3$, 2 diastereomers): δ=21.2 (2Ts-CH$_3$), 34.1 (C4a′), 34.2 (2CH$_3$), 34.2 (C4a′), 37.4 (C2′), 38.4 (C2′), 44.5 (C4′), 44.7 (C4′), 60.4 (C1′), 61.5 (C1′), 71.0 (CH$_2$), 71.1 (CH$_2$), 71.5 (C6′), 71.6 (C6′), 73.1 (CH$_2$), 73.2 (CH$_2$), 79.6 (C3′), 81.0 (C3′), 88.5 (-CH=), 88.6 (-CH=), 108.7 (TO-ArCH), 109.5 (TO-ArCH), 111.8 (2TO-ArCH), 115.9 (1TO-ArCH), 116.9 (1TO-ArCH), 121.9 (1TO-ArCH), 122.0 (1TO-ArCH), 123.9 (1TO-ArCH), 124.0 (1TO-ArCH), 124.2 (1TO-ArC$_q$), 124.3 (1TO-ArC$_q$), 124.5 (2TO-ArC′$_q$), 126.1 (4Ts-ArCH), 126.2 (1TO-ArCH), 126.4 (1TO-ArCH), 126.6 (1TO-ArCH), 126.8 (1TO-ArCH), 127.1 (1TO-ArCH), 127.5 (2TO-ArCH), 127.6 (4Ts-ArCH, 4Bn-ArCH), 127.6 (4Bn-ArCH), 128.1 (TO-ArCH), 128.2 (2Bn-ArCH), 128.3 (2Bn-ArCH), 128.3 (4Bn-ArCH), 128.4 (4Bn-ArCH), 131.1 (1TO-ArCH), 132.5 (1TO-ArCH), 137.1 (Bn-ArC$_q$), 137.4 (Bn-ArC$_q$) 137.9 (Bn-ArC$_q$), 138.1 (2TO-ArC$_q$), 138.2 (Bn-ArC$_q$), 138.6 (2Ts-ArCH), 139.9 (1TO-ArC$_q$), 140.0 (1TO-ArC$_q$), 140.3 (1TO-ArCH), 140.4 (1TO-ArCH), 139.9 (2TO-ArC$_q$), 140.0 (2TO-ArC$_q$), 140.4 (1TO-ArCH), 140.3 (1TO-ArCH), 144.7 (2Ts-ArCH), 148.2 (1TO-ArC$_q$), 148.3 (1TO-ArC$_q$), 159.5 (1TO-ArC$_q$), 159.6 ppm (1TO-ArC$_q$); HRMS (ESI): *m/z* calcd: 585.2570 [C$_{38}$H$_{37}$N$_2$O$_2$S]$^+$, found: 585.2568.

4a′-Carba-α/β-(D)-2′-deoxyribofuranose(TO) (4): Under argon, BBr_3 (2.61 g, 1.02 mL, 10.4 mmol) was added dropwise to a cooled (0 °C) solution of **3** (1.58 g, 2.09 mmol) in dry CH_2Cl_2 (60 mL). Complete addition resulted in a colorless suspension. Saturated $NaHCO_3$ (aq.) solution (150 mL) was added after 10 min. After 30 min the precipitate was collected, dried under reduced pressure to give a red powder, which was used without further purification. R_f=0.15 (CH_2Cl_2/MeOH/NEt_3 90:10:0.1, *v/v/v*); ^{1}H NMR (300 MHz, [D$_6$]DMSO, 2 diastereomers in 1:1.5 ratio): δ=1.73 (m, 1H), 2.09 (m, 4H), 2.26 (m, 4H) 2.57 (m, 1H), 3.52 (m, 4H; 2H5′a, 2H5′b), 3.96 (s, 6H; 2CH$_3$), 4.12 (m, 2H; 2H3′), 5.45 (m, 2H; 2H1′), 6.82 (s, 2H; 2CH), 7.32 (m, 4H; 4TO-H), 7.53 (m, 2H; 2TO-H), 7.70 (m, 4H; 4TO-H), 7.98 (m, 4H; 4TO-H), 8.21 (m, 2H; 2TO-H), 8.69 (m, 1H; TO-H), 8.75 (m, 2H; TO-H), 8.84 ppm (m, 1H; TO-H); ^{13}C NMR (75 MHz, [D$_6$]DMSO, 2 diastereomers): δ=33.8 (N$^+$-CH$_3$), 33.8 (N$^+$-CH$_3$), 34.0 (2C4a′), 40.2 (C2′), 40.6 (C2′), 48.8 (C4′), 49.3 (C4′), 59.8 (C1′), 60.4 (C1′), 61.8 (C5′), 61.9 (C5′), 70.9 (C3′), 71.9 (C3′), 87.8 (TO-CH=), 87.9 (TO-CH=), 108.1 (2TO-ArCH), 112.8 (1TO-ArCH), 114.0 112.8 (1TO-ArCH), 117.8 (1TO-ArCH), 117.9 (1TO-ArCH), 122.7 (1TO-ArCH), 122.8 (1TO-ArCH), 123.7 (2TO-ArC$_q$), 124.1 (1TO-ArC$_q$), 124.1 (1TO-ArC$_q$), 124.2 (1TO-ArCH), 124.3 (1TO-ArCH), 125.7 (2TO-ArCH), 126.6 (1TO-ArCH), 126.6 (1TO-ArCH), 128.0 (2TO-ArCH), 133.0 (1TO-ArCH), 133.1 (1TO-ArCH), 137.5 (1TO-ArC$_q$), 137.7 (1TO-ArC$_q$), 140.1 (1TO-ArCH), 140.2 (2TO-ArC$_q$), 140.9 (1TO-ArCH), 147.9 (1TO-ArC$_q$), 147.9 (1TO-ArC$_q$), 159.6 (1TO-ArC$_q$), 159.7 ppm (1TO-ArC$_q$); (ESI): *m/z* calcd: 405.1631 [C$_{24}$H$_{25}$N$_2$O$_2$S]$^+$, found: 405.1628.

4a′-Carba-α/β-(D)-5′-DMT-2′-deoxyribofuranose(TO) (5β/α): KPF_6 (769 mg, 4.18 mmol) was added to a suspension of compound **4** (1.58 g, 2.09 mmol) in dry pyridine (100 mL) under argon. The turbid solution became clear, and EtN*i*Pr$_2$ (2.70 g, 20.9 mmol, 3.45 mL) and DMTrCl (3.40 g, 10.0 mmol) were added. After 16 h the mixture was filtered. The filtrate was concentrated. The residue was dissolved in CH_2Cl_2, washed three times with saturated $NaHCO_3$ (aq.), dried ($MgSO_4$), filtered, and concentrated. The residue was purified by flash column chromatography in order to separate diastereomers, which were obtained as red solids (**5β**, 906 mg, 1.06 mmol, 51%; **5α**, 604 mg, 0.71 mmol, 34%). R_f=0.80 (CH_2Cl_2/MeOH/NEt_3 90:10:0.1, *v/v/v*).

4a′-Carba-β-(D)-5′-DMT-2′-deoxyribofuranose(TO) (5β): ^{1}H NMR (400 MHz, CD_3CN): δ=1.67 (m, 1H; H4a′a), 2.29 (m, 3H; H2′a, H2′b, H4′), 2.63 (m, 1H; H4a′b), 3.22 (m, 2H; H5′a, H5′b), 3.72 (s, 6H; 2DMT-OCH3), 3.80 (s, 3H; TO-H18), 4.32 (m, 1H; H3′), 5.32 (m, 1H; H1′), 6.63 (s, 2H; TO-H10), 6:84 (m, 4H; 4DMT-ArH), 7.18 (m, 1H; TO-H2), 7.23 (m, 1H; DMT-ArH), 7.30 (m, 6H; 6DMT-ArH), 7.34 (m, 1H; TO-H14), 7.43 (m, 3H; TO-H16, 2DMT-ArH), 7.51 (m, 1H; TO-H15), 7.66 (m, 1H; TO-H6), 7.78 (m, 1H; TO-H13), 7.87 (m, 1H; TO-H7), 7.98 (m, 1H; TO-H8), 8.27 (m, 1H; TO-H1), 8.48 ppm (m, 1H; TO-H5); ^{13}C NMR (100 MHz, CD_3CN): δ=34.5 (TO-H18), 35.2 (C4a′), 41.1 (C2′), 48.0 (C4′), 55.8 (2DMT-OCH$_3$), 61.0 (C1′), 64.5 (C5′), 73.0 (C3′), 86.9 (DMT-Cq), 88.8 (TO-C10), 109.3 (TO-C2), 113.4 (TO-C16), 114.0 (2DMT-ArCH), 114.0 (2DMT-ArCH), 118.7 (TO-C8), 123.4 (TO-C13), 125.1 (TO-C12), 125.4 (TO-C4), 125.5 (TO-C14), 126.2 (TO-C5), 127.7 (TO-C6), 127.8 (DMT-ArCH), 128.8 (2DMT-ArCH), 129.0 (2DMT-ArCH), 129.1 (TO-C15), 130.9 (2DMT-ArCH), 130.9 (2DMT-ArCH), 134.1 (TO-C7), 137.1 (DMT-ArC$_q$), 137.2 (DMT-ArC$_q$), 139.0 (TO-C9), 140.2 (TO-C1), 141.4 (1TO-C17), 146.1 (DMT-ArC$_q$), 149.5 (TO-C3), 159.5 (2DMT-ArC$_q$), 161.3 ppm (TO-C11); HRMS (ESI): *m/z* calcd: 707.2938 [C$_{45}$H$_{43}$N$_2$O$_4$S]$^+$, found: 707.2928.

4a′-Carba-α-(D)-5′-DMT-2′-deoxyribofuranose(TO) (5α): ^{1}H NMR (400 MHz, CD_3CN): δ=2.05 (m, 1H; H2′a), 2.19 (m, 2H; H4a′a, H4a′b), 2.39 (m, 1H; H4′), 2.61 (m, 1H; H2′b), 3.18 (m, 2H; H5′a, H5′b), 3.76 (s, 3H; TO-H18), 3.77 (s, 6H; 2DMT-OCH$_3$), 4.28 (m, 1H; H3′), 5.19 (m, 1H; H1′), 6.56 (s, 2H; TO-H10), 6:89 (m, 4H; 4DMT-ArH), 7.21 (m, 1H; TO-H2), 7.27 (m, 2H; DMT-ArH, TO-H14), 7.35 (7H, m, 6DMT-ArH, TO-H16), 7.47 (m, 3H; TO-H15, 2DMT-ArH), 7.61 (m, 1H; TO-H6), 7.71 (m, 1H; TO-H13), 7.78 (m, 1H; TO-H7), 7.84 (m, 1H; TO-H8), 8.42 (m, 1H; TO-H5), 8.57 ppm (m, 1H; TO-H1); ^{13}C NMR (100 MHz, CD_3CN): δ=34.4 (TO-C18), 35.5 (C4a′), 41.5 (C2′), 48.6 (C4′), 55.9 (2DMT-OCH$_3$), 61.9 (C1′), 65.1 (C5′), 74.3 (C3′), 86.9 (DMT-C$_q$), 88.6 (TO-C10), 109.3 (TO-C2), 113.3 (TO-C16), 114.0 (4DMT-ArCH), 118.5 (TO-C8), 123.3 (TO-C13), 125.1 (TO-C12), 125.4 (TO-C4), 125.4 (TO-C14), 126.2 (TO-C5), 127.5 (TO-C6), 127.8 (DMT-ArCH), 128.8 (2DMT-ArCH), 129.0 (2DMT-ArCH), 129.0 (TO-C15), 131.0 (4DMT-ArCH), 133.9 (TO-C7), 137.1 (DMT-ArC$_q$), 137.1 (DMT-ArC$_q$), 138.9 (TO-C9), 141.3 (1TO-C17), 141.4 (TO-C1), 146.3 (DMT-ArC$_q$), 149.4 (TO-C3), 159.6 (2DMT-ArC$_q$), 161.1 ppm (TO-C11); HRMS (ESI): *m/z* calcd: 707.2938 [C$_{45}$H$_{43}$N$_2$O$_4$S]$^+$, found: 707.2930.

Preparation of phosphoramidites: Nucleoside (0.5 mmol) and 2-cyanoethyl *N*,*N*-diisopropylchlorophosphoramidite (1.25 mmol, 296 mg, 279 μL) were added to a solution of freshly distilled EtN*i*Pr$_2$ (2.5 mmol, 323 mg, 413 μL) in dry CH_2Cl_2 (10 mL). After 1 h of stirring at room temperature the reaction was quenched by addition of saturated $NaHCO_3$ (aq.). The organic layer was separated and washed twice with saturated $NaHCO_3$ (aq.), dried over $MgSO_4$, and filtered. The filtrate was collected, and the volatiles were removed at reduced pressure. The crude product was dissolved in dry CH_3CN to a concentration of 0.1 M and transferred to an ABI-style reagent bottle for subsequent use in DNA synthesis.

DNA synthesis, work-up, and purification: The DNA FIT probes were assembled by using a model 3400 synthesizer (Applied Biosystems) and by the phosphoramidite method (above). CPGs (1 μmol, pore size 500 Å) were purchased from Proligo (Sigma Aldrich) and Link Technologies (Bellshill, UK), and DNA synthesis reagents (dry CH_3CN, trichloroacetic acid (3% in CH_2Cl_2), acetic anhydride in 2,6-lutidin/THF (1:1:8), 1-methylimidazole (16% in THF), and iodine in water/pyridine/THF (3:2:20:75)) were purchased from Roth or Link Technologies. The phosphoramidites dT, dA^{Bz}, dC^{Bz}, and dG^{DMF} (0.1 M) were used in dry CH_3CN. Activator (5-benzylmercapto-1*H*-tetrazole (BMT)) was purchased from emp Biotech (Berlin, Germany) and used as a 0.25 M solution in dry CH_3CN. The synthesized phosphoramidites were used at 0.1 M in dry CH_3CN. The quality of each coupling step was monitored by measuring the conduc-

tivity of DMT cleavage solutions. The synthesizer was programmed to yield oligomers carrying the terminal DMT protective group, "trityl-on". After synthesis, the resulting CPGs were dried under reduced pressure and then transferred to 2 mL Eppendorf tubes. Aqueous ammonia (1 mL, 32%) was added, and the tubes were shaken for 2 h at 55 °C. Subsequently, the tubes were centrifuged and the supernatant was collected. The volatiles were removed at reduced pressure, and the samples were dissolved in TEAA buffer (0.1 M, pH 7). The crude product was further purified by RP-HPLC. Afterwards, the DMTr group was removed by treatment with AcOH (50% aq.) for 30 min. The reaction mixtures were neutralized with NEt_3, and the crude product was again purified by RP-HPLC. The resulting oligomers were concentrated to an overall volume of 0.5 mL and desalted by using NAP-5 Sephadex columns (GE Healthcare). Finally, the oligomers were freeze dried, and the residues were dissolved in water (Millipore) to a final concentration of 0.1 mM. Identity and purity were determined by using analytical RP-HPLC or UPLC and MALDI-TOF or ESI(−)-Q-TOF mass spectroscopy.

Fluorescence spectroscopy: Fluorescence emission spectra were measured by using a Cary Eclipse (Varian/Agilent Technologies) with 10 mm quartz cuvettes and phosphate buffer (Na_2HPO_4 (10 mM, pH 7), NaCl (100 mM)) and background corrected. DNA FIT probes and target DNA/RNA were added as specified. Spectra were recorded upon constant emission. After addition of DNA conjugate (DNA or RNA stock solutions), the samples were heated to 85 °C (2 min), and cooled to 37 °C. Prior to measurement, samples were allowed to equilibrate for 2 min. For TO conjugates: λ_{ex} = 485 nm, λ_{em} = 500–700 nm; for BO conjugates: λ_{ex} = 440 nm, λ_{em} = 455–700 nm. The spectra were the averages of five measurement cycles and blank corrected. For measurements in cell lysate we used lysate of 10^5 MDCK cells in lysis buffer (Tris·HCl (50 mM, pH 7.4), NaCl (150 mM), nonyl phenoxypolyethoxylethanol (detergent; 0.8%)). Degradation experiments were performed with DNase I (Sigma–Aldrich) at 37 °C. For complete digestion, the specified probe (0.675 nmol) was treated with freshly prepared DNase I (40 μL, 0.44 mg mL^{-1} in PBS) for 1 h at 37 °C. Denaturation of DNase I was achieved by heating to 80 °C for 15 min. Completion of digestion was confirmed by addition of target RNA and the resulting lack of a fluorescence response. Degraded probes were added to either PBS or cell media. Fluorescence measurements were carried out at a final concentration of 1 μM in the specified medium. For time-dependent measurements of fluorescence, TO- and BO-containing probes were added together in the same cuvette. BO: λ_{ex} = 460 nm, λ_{em} = 480 nm, TO: λ_{ex} = 485 nm or λ_{ex} = 515 nm, λ_{em} = 535 nm; TAMRA: λ_{ex} = 540 nm, λ_{em} = 580 nm. Neither samples nor probes were denaturated prior to use. For time-dependent fluorescence with DNase I, probes (0.15 nmol each) were jointly added to PBS buffer and single-strand fluorescence was measured for 3 min (I_0), followed by addition of freshly prepared DNase I (10 μL, 0.05 mg mL^{-1}) to a final concentration of 0.1 μM of each probe (150 μL total volume). After 32 min, target RNA (**RNA2**, 0.75 nmol) was added.

qPCR: PCR was performed on a iQ thermocycler (BioRad, Hercules, CA) with PCR Master Mix S (PEQLAB Biotechnologie, Erlangen, Germany), containing argon-saturated water, reaction buffer high specificity S, enhancer (solution P), magnesium chloride (2.5 mM), dNTP-mix long range (200 μM dNTPs), forward primer (CTTGGT CAGCAA GTGCAT GT, 400 nM; Biotez, Berlin, Germany), reverse primer (CTCGGG CCATCA GTCATT AT, 400 nM), Taq DNA polymerase (1 U; PEQLAB Biotechnologie) and of DNA template-solution (1 μL) (100 ng μL^{-1}, 10 ng μL^{-1}, 1 ng μL^{-1}, 100 pg μL^{-1}, 10 pg μL^{-1}, 1 pg μL^{-1} and 100 fg μL^{-1}, 10 fg μL^{-1}). In the no-template control (NTC), DNA was replaced with water. DNA template (10 ng μL^{-1}) obtained from non-infected cells was used as further control. The solutions were prepared on ice. Each reaction mixture (3 × 20 μL (triple experiments)) was transferred to a well plate, sealed with a plastic foil, and centrifuged to remove air bubbles. The temperature protocol of the PCR included initial denaturation (95 °C, 2 min), followed by 30 cycles of denaturation (95 °C, 10 s), primer annealing (57.5 °C, 30 s), and elongation (72 °C, 20 s), and finally cooling to 4 °C. Fluorescence readout was performed at the annealing temperature. Target sequence: H1N1A/PR/8 neuraminidase (nt 496–684).[31]

Acknowledgements

Support by a fellowship of the Fonds der Chemischen Industrie for F.H. is appreciated. We wish to thank Dr. Susann Kummer, Matthias Schade and Prof. Dr. Andreas Herrmann, Department of Biology, Humboldt University Berlin, Invalidenstrasse 42, 10115 Berlin (Germany) for providing MDCK cell lysate and cDNA.

Keywords: fluorescence · hybridization probes · molecular beacon · RNA · thiazole orange

[1] E. T. Kool, *Acc. Chem. Res.* **2002**, *35*, 936–943.
[2] M. J. Rist, J. P. Marino, *Curr. Org. Chem.* **2002**, *6*, 775–793.
[3] a) Y. L. Jiang, J. T. Stivers, *Biochemistry* **2002**, *41*, 11236–11247; b) C. Beuck, I. Singh, A. Bhattacharya, W. Hecker, V. S. Parmar, O. Seitz, E. Weinhold, *Angew. Chem.* **2003**, *115*, 4088–4091; *Angew. Chem. Int. Ed.* **2003**, *42*, 3958–3960; c) M. M. Somoza, D. Andreatta, C. J. Murphy, R. S. Coleman, M. A. Berg, *Nucleic Acids Res.* **2004**, *32*, 2494–2507.
[4] R. W. Sinkeldam, N. J. Greco, Y. Tor, *Chem. Rev.* **2010**, *110*, 2579–2619.
[5] a) V. L. Malinovskii, D. Wenger, R. Häner, *Chem. Soc. Rev.* **2010**, *39*, 410–422; b) T. J. Bandy, A. Brewer, J. R. Burns, G. Marth, T. Nguyen, E. Stulz, *Chem. Soc. Rev.* **2011**, *40*, 138–148.
[6] a) K. Nakatani, *ChemBioChem* **2004**, *5*, 1623–1633; b) R. T. Ranasinghe, T. Brown, *Chem. Commun.* **2005**, 5487–5502; c) A. P. Silverman, E. T. Kool in *Advances in Clinical Chemistry, Vol. 43* (Ed.: G. S. Makowski), Academic Press, San Diego, **2007**, pp. 79–115.
[7] a) C. A. Foy, H. C. Parkes, *Clin. Chem.* **2001**, *47*, 990–1000; b) I. M. Mackay, K. E. Arden, A. Nitsche, *Nucleic Acids Res.* **2002**, *30*, 1292–1305.
[8] a) S. Tyagi, *Nat. Methods* **2009**, *6*, 331–338; b) B. A. Armitage, *Curr. Opin. Chem. Biol.* **2011**, *15*, 806–812.
[9] a) A. P. Silverman, E. T. Kool, *Trends Biotechnol.* **2005**, *23*, 225–230; b) C. J. Yang, K. Martinez, H. Lin, W. Tan, *J. Am. Chem. Soc.* **2006**, *128*, 9986–9987.
[10] A. K. Chen, M. A. Behlke, A. Tsourkas, *Nucleic Acids Res.* **2007**, *35*, e105.
[11] a) T. Ishiguro, J. Saitoh, H. Yawata, M. Otsuka, T. Inoue, Y. Sugiura, *Nucleic Acids Res.* **1996**, *24*, 4992–4997; b) A. Okamoto, K. Tainaka, Y. Ochi, K. Kanatani, I. Saito, *Mol. Biosyst.* **2006**, *2*, 122–127; c) N. Svanvik, A. Ståhlberg, U. Sehlstedt, R. Sjöback, M. Kubista, *Anal. Biochem.* **2000**, *287*, 179–182.
[12] a) O. Seitz, F. Bergmann, D. Heindl, *Angew. Chem.* **1999**, *111*, 2340–2343; *Angew. Chem. Int. Ed.* **1999**, *38*, 2203–2206; b) O. Köhler, O. Seitz, *Chem. Commun.* **2003**, 2938–2939; c) O. Köhler, D. V. Jarikote, O. Seitz, *ChemBioChem* **2005**, *6*, 69–77.
[13] a) L. G. Lee, C.-H. Chen, L. A. Chiu, *Cytometry* **1986**, *7*, 508–517; b) J. Nygren, N. Svanvik, M. Kubista, *Biopolymers* **1998**, *46*, 39–51; c) V. Karunakaran, J. L. Pérez Lustres, L. Zhao, N. P. Ernsting, O. Seitz, *J. Am. Chem. Soc.* **2006**, *128*, 2954–2962.
[14] D. V. Jarikote, N. Krebs, S. Tannert, B. Röder, O. Seitz, *Chem. Eur. J.* **2007**, *13*, 300–310.
[15] E. Socher, D. V. Jarikote, A. Knoll, L. Röglin, J. Burmeister, O. Seitz, *Anal. Biochem.* **2008**, *375*, 318–330.

[16] S. Kummer, A. Knoll, E. Socher, L. Bethge, A. Herrmann, O. Seitz, *Angew. Chem.* **2011**, *123*, 1972 – 1975; *Angew. Chem. Int. Ed.* **2011**, *50*, 1931 – 1934.
[17] a) A. Tonelli, T. Tedeschi, A. Germini, S. Sforza, R. Corradini, M. C. Medici, C. Chezzi, R. Marchelli, *Mol. Biosyst.* **2011**, *7*, 1684 – 1692; b) A. G. Torres, M. M. Fabani, E. Vigorito, D. Williams, N. Al-Obaidi, F. Wojciechowski, R. H. Hudson, O. Seitz, M. J. Gait, *Nucleic Acids Res.* **2012**, *40*, 2152 – 2167; c) Y. Kam, A. Rubinstein, A. Nissan, D. Halle, E. Yavin, *Mol. Pharm.* **2012**, *9*, 685 – 693.
[18] P. E. Nielsen, M. Egholm, R. H. Berg, O. Buchardt, *Science* **1991**, *254*, 1497 – 1500.
[19] U. Asseline, M. Chassignol, Y. Aubert, V. Roig, *Org. Biomol. Chem.* **2006**, *4*, 1949 – 1957.
[20] S. Berndl, H.-A. Wagenknecht, *Angew. Chem.* **2009**, *121*, 2454 – 2457; *Angew. Chem. Int. Ed.* **2009**, *48*, 2418 – 2421.
[21] S. Ikeda, T. Kubota, M. Yuki, H. Yanagisawa, S. Tsuruma, A. Okamoto, *Org. Biomol. Chem.* **2010**, *8*, 546 – 551.
[22] L. Bethge, I. Singh, O. Seitz, *Org. Biomol. Chem.* **2010**, *8*, 2439 – 2448.
[23] S. Jessel, E. Hense, C. Meier, *Nucleosides Nucleotides Nucleic Acids* **2007**, *26*, 1181 – 1184.
[24] M. H. Caruthers, A. D. Barone, S. L. Beaucage, D. R. Dodds, E. F. Fisher, L. J. McBride, M. Matteucci, Z. Stabinsky, J.-Y. Tang, *Methods Enzymol.* **1987**, *154*, 287 – 313.
[25] MDCK beta-actin; NCBI reference sequence: NM_001195845.1.
[26] H1N1 neuraminidase APR8; GenBank sequence: CY084184.1.
[27] W. Wang, Z.-Q. Cui, H. Han, Z.-P. Zhang, H.-P. Wei, Y.-F. Zhou, Z. Chen, X.-E. Zhang, *Nucleic Acids Res.* **2008**, *36*, 4913 – 4928.
[28] S. Tyagi, F. R. Kramer, *Nat. Biotechnol.* **1996**, *14*, 303 – 308.
[29] L. Bethge, D. V. Jarikote, O. Seitz, *Bioorg. Med. Chem.* **2008**, *16*, 114 – 125.
[30] C. Holzhauser, H.-A. Wagenknecht, *Angew. Chem.* **2011**, *123*, 7406 – 7410; *Angew. Chem. Int. Ed.* **2011**, *50*, 7268 – 7272.
[31] D. J. French, C. L. Archard, T. Brown, D. G. McDowell, *Mol. Cell. Probes* **2001**, *15*, 363 – 374.
[32] A. Okamoto, *Chem. Soc. Rev.* **2011**, *40*, 5815 – 5828.
[33] N. Moran, D. M. Bassani, J.-P. Desvergne, S. Keiper, P. A. S. Lowden, J. S. Vyle, J. H. R. Tucker, *Chem. Commun.* **2006**, 5003 – 5005.

Received: June 12, 2012
Published online on ■■ ■■, 0000

FIT for the right track: The fluorescence response of DNA probes that contain a single thiazole orange (TO) "base" is specific for complementary RNA and DNA targets. Strong fluorescence enhancements are obtained at varied temperatures and in challenging media such as cell lysates.

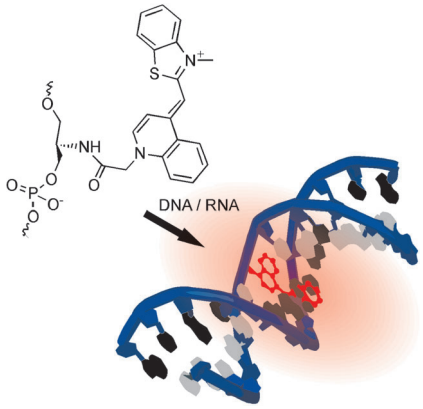

*F. Hövelmann, L. Bethge, O. Seitz**

■■ – ■■

Single Labeled DNA FIT Probes for Avoiding False-Positive Signaling in the Detection of DNA/RNA in qPCR or Cell Media

